Supporting Information

Chicas et al. 10.1073/pnas.1119836109

SI Materials and Methods

Retroviral Vectors. The following retroviral vectors were used in this study: pWZL-Hygro (H-rasV12), pWZL-Blasticidin (H-rasV12), pLNCX2-neo (ER:rasv12) (1). shRNAs targeting retinoblastoma (RB) were previously described (2). shRNAs targeting Jarid1a and Jarid1b were generated using the method previously described (3). Briefly, the 10 top-scoring siRNA predications were obtained using BIOPREDsi and the siRNA was incorporate into the Mir-30 backbone (4). The polycistronic shRNA vectors were cloned in two steps as described (2). The Jarid1a cDNA was a gift from Ed Harlow (Massachusetts General Hospital, Charlestown, MA; ref. 5) and was subcloned into MSCVpuro (Clontech). Mutants were made using a QuikChange II Site-Directed Mutagenesis Kit (Stratagene). The infected population was selected using either 2 μg/mL Puromycin (Sigma) for 2 d, 500 μg/mL Neomycin for 3 d, 75 μg/mL Hygromycin B (Roche) for 3 d, or Blastacidin (10 μg/mL for 4 d).

Isolation of Chromatin-Bound Proteins. Cells were resuspended in buffer A [mM Hepes (pH 7.9), 10 mM KCl, 1.5 mM $MgCl_2$, 0.34 M sucrose, 10% (vol/vol) glycerol, 1 mM DTT, protease inhibitor mixture (Complete, Roche), 0.1 mM phenylmethylsulphonyl fluoride]. Digitonin (Sigma, 0.3 mg/mL) was added and the cells were incubated for 10 min on ice. Nuclei were collected by low-speed centrifugation (4 min, 1,300 × *g*, 4 °C) and supernatants were isolated as cytoplasmic factions. Nuclei were washed once in buffer A and lysed in buffer B (3 mM EDTA, 0.2 mM EGTA, 1 mM DTT, protease inhibitors as described above). After being incubated on ice for 30 min with occasional vortexing, the insoluble chromatin factions were isolated by low-speed centrifugation and supernatants served as nucleoplasmic fractions. After vigorous washing with buffer B, the chromatin pellets were resuspended in immunoprecipitation buffer (20 mM Tris pH 8.0, 1 mM EDTA, 0.5 mM EGTA, 200 mM NaCl, 0.5% Triton X, 0.05% deoxycholate, 0.1% IGE-PAL, 1 mM PMSF Protease Inhibitor) and briefly sonicated to solubilize the chromatin. For immunoblotting, the chromatin pellet was solubilized with DNase I (Roche) [2 × 103 units/mL DNase I, 20 mM Tris (pH7.5), 10 mM $MgCl_2$] for 1 h on ice. Samples were analyzed by SDS/PAGE.

Antibodies. The following antibodies were used: Anti-Jarid1a (# 3876S, Cell Signaling; 1:1,000), anti-Jarid1b (# 3273S, Cell Signaling; 1:1,000), anti-H3K4me3 (# 05–745, Millipore; 1:500), anti-RB antibody (G3-245, Pharmingen; 1:1,000) together with XZ-55 hybridoma supernatant (1:100), anti-Histone H3 (sc-8654, Santa Cruz; 1:250), anti-p16INK4a (H-156, Santa Cruz; 1:250), anti-p53 (DO-1, Oncogene; 1:1,000), anti-Cyclin A (Sigma; 1:1,000), anti Cyclin B (Cell Signaling; 1:1,000), anti–α-tubulin (B-5–1-2, Sigma; 1:5,000), anti-Actin (ac-15, Sigma; 1:10,000), anti-MCM3 [Bruce Stillman (Cold Spring Harbor Laboratory, Cold Spring Harbor, NY), 1:1,000], anti-MCM2 (Bruce Stillman, 1:1,000), antiproliferating cell nuclear antigen (Bruce Stillman, 1:1,000), anti-ras (Calbiochem; 1:500), anti-p21 (C-19, Santa Cruz; 1:200), H3K4me2 (Upstate; 05–1388), H3K4me3 (Upstate; 05–745), H3K27me3 (Upstate; 07–449), H4K20me1 (Upstate; 05–735), H4K20me3 (Upstate; 07–463), H3K9ac (Upstate; 07–352), H3K18ac (Upstate; 07–354), H3K27ac (Upstate; 07–360), and H4ac (Upstate; 06–866).

Deep-Sequencing ChIP Analysis. We used MACS [model-based analysis for deep-sequencing ChIP (ChIP-seq)] (6) to find H3K4me3-enriched regions compared with the IgG control with default parameter settings and a significance threshold ($P \leq 10–5$) and false-discovery rate threshold of 1%. We associated H3K4me3-enriched regions to a target gene if it locates within the region from 1-kb upstream of the transcription start site to the transcription end site of the gene. The gene coordinates were extracted according to refseq gene annotation (hg18) downloaded from the University of California at Santa Cruz genome browser.

1. Young AR, et al. (2009) Autophagy mediates the mitotic senescence transition. *Genes Dev* 23:798–803.
2. Chicas A, et al. (2010) Dissecting the unique role of the retinoblastoma tumor suppressor during cellular senescence. *Cancer Cell* 17:376–387.
3. Zuber J, et al. (2011) Toolkit for evaluating genes required for proliferation and survival using tetracycline-regulated RNAi. *Nat Biotechnol* 29:79–83.
4. Silva JM, et al. (2005) Second-generation shRNA libraries covering the mouse and human genomes. *Nat Genet* 37:1281–1288.
5. Fattaey AR, et al. (1993) Characterization of the retinoblastoma binding proteins RBP1 and RBP2. *Oncogene* 8:3149–3156.
6. Zhang Y, et al. (2008) Model-based analysis of ChIP-Seq (MACS). *Genome Biol* 9:R137.

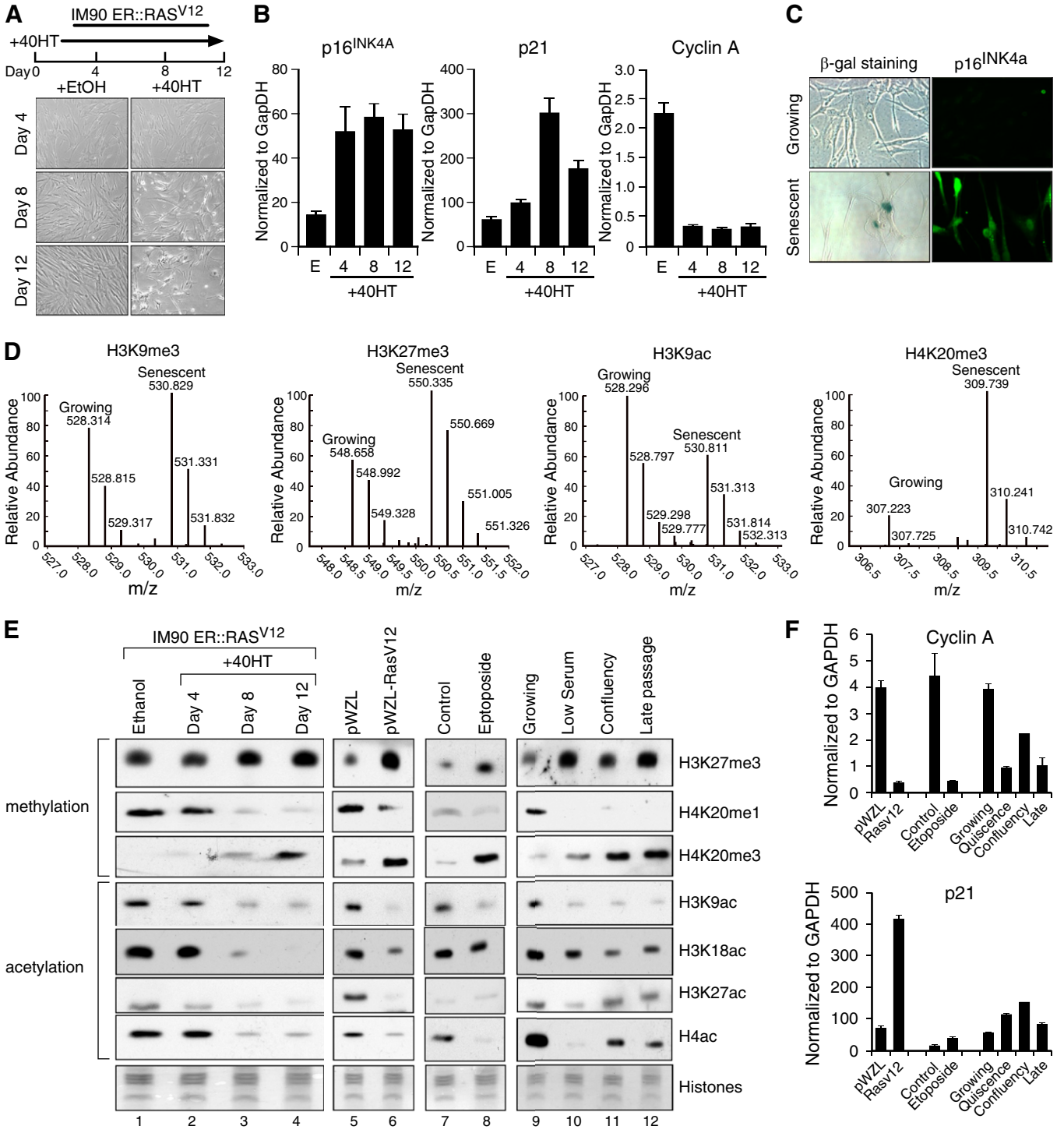

Fig. S1. (*A*) Micrographs documenting the morphological changes triggered by ER::Ras^{V12}-induced senescence of IMR90 cells. Magnification: 10×. (*B*) Histograms documenting the mRNA increase in senescence markers (p16, p21) and decrease of Cyclin A mRNA in senescent cells from *A*. E, ethanol-treated controls; 4, 8, and 12 represent days treated with 4OHT. (*C*) Micrographs documenting the expression of p16 and increased senescence-associated β-galactosidase (SA-β-gal) activity in senescent cells. Magnification: 20×. (*D*) Mass spectrum of quantitative proteomics comparing growing and senescent cells for H3K9me3, H3K27me3, H3K9ac, and H4K20me3. Doubly charged peaks correspond to propionylated peptides. Note the increased levels of H3K9me3, H3K27me3, and H4K20me3 during senescence; the levels of H3K9ac are higher in growing cells. One of three independent technical replicates is shown. (*E*) Immunoblot validation of quantitative MS (qMS). IMR90 ER::Ras^{V12} cells control treated with ethanol (lane 1) or 4OHT for the indicated time (lanes 2–4), IMR90 infected with a vector control (lane 5) or a vector expressing activated Ras ^{V12} (lane 6), treated with DMSO (lane 7) or 50 μM etoposide (lane 8), growing IMR90 (lane 9), low serum-induced quiescence (lane 10), confluency-induced quiescence (lane 11), and replicative senescence (lane 12). Core histones were used as loading control. (*F*) Histograms documenting the **m**RNA expression of Cyclin A and p21 for the conditions shown in *E*.

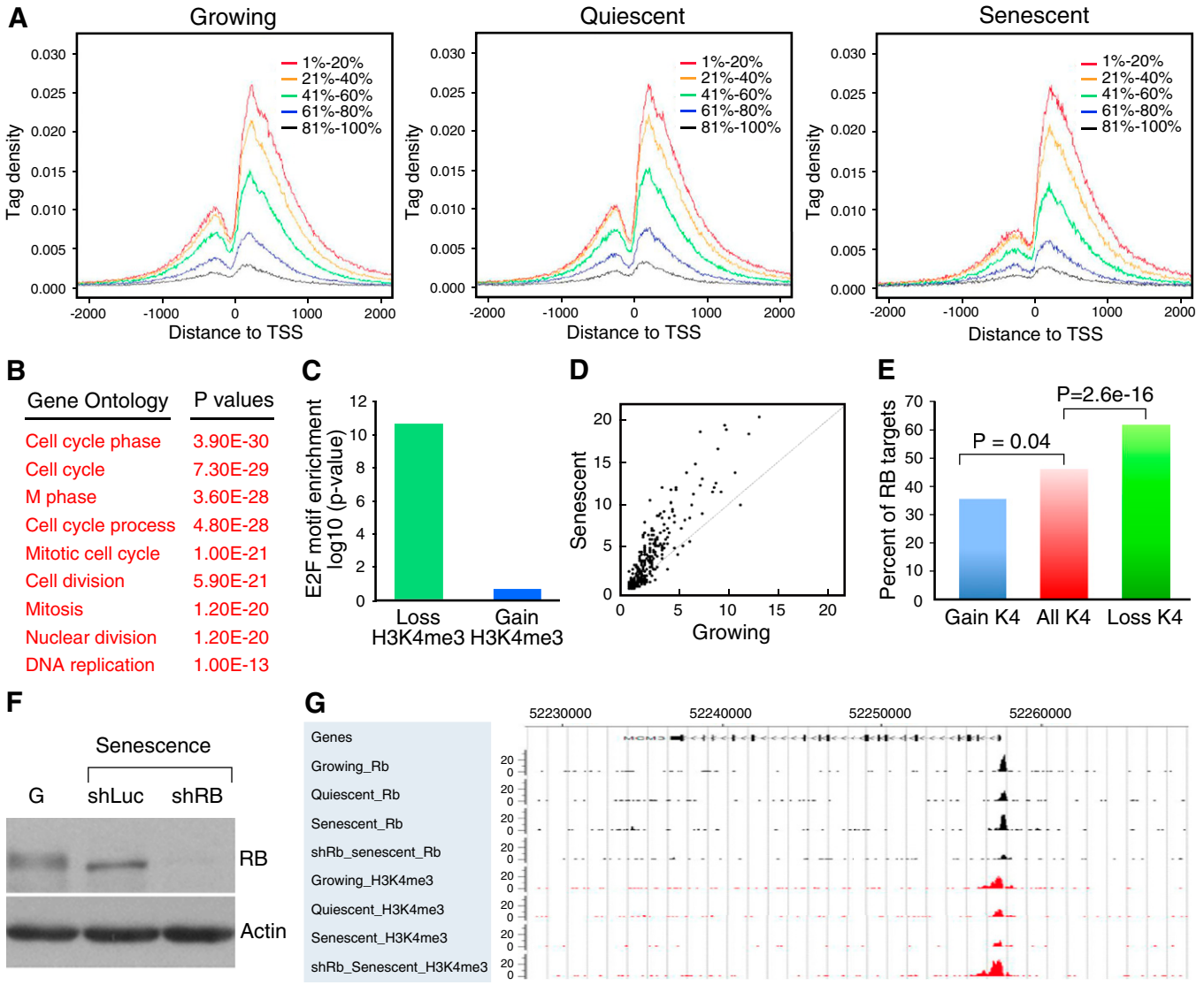

Fig. S2. (*A*) Profiles of H3K4me3 around the transcription start site of genes with different expression level in growing, quiescent, or senescent cells. Genes were separated into five equal-sized groups according to their expression level (descending order, 1–20% with highest expression level and 81–100% with lowest expression level). (*B*) Gene Ontology categories of the top nine scoring gene sets associated with loss of H3K4me3. (*C*) E2F binding sites are enriched in the genes associated with loci that showed loss of H3K4 methylation. "Loss K4" are regions that show significantly less reads in senescent than in growing cells. "Gain K4" are regions that show significantly more reads in senescent that in growing cells. "All K4" represents the whole set of genes that have a significant H3K4me3-enriched region. To determine the regions that lose or gain H3K4me3 in senescent cells, the number of ChIP-seq reads located in each H3K4me3-enriched region were compared between growing and senescent cells and the significance of the difference calculated by χ^2 analysis. (*D*) RB binds with higher affinity to E2F target genes in senescent cells. The plot shows the normalized RB ChIP-seq intensity at the curated E2F target gene-promoter region (−700 bp to +300 bp relative to transcription start site) in growing and senescent cells. Each dot represents an E2F target gene promoter. The *x* axis and *y* axis show per-million reads count of RB ChIP-seq experiment in growing and senescent, respectively. (*E*) Correlation between RB binding and loss of H3K4me3 in senescent cells. (*F*) Immunoblot documenting efficient suppression of RB by the shRNA using in this study. (*G*) Genome-browser view documenting the loss of the H3K4me3 modification at the MCM3 gene in senescent (Senescent_H3K4me3) cells but not growing (Growing_H3K4me3), quiescent (Quiescent_H3K4me3), or RB-deficient senescent (shRb_Senescent_H3K4me3) cells.

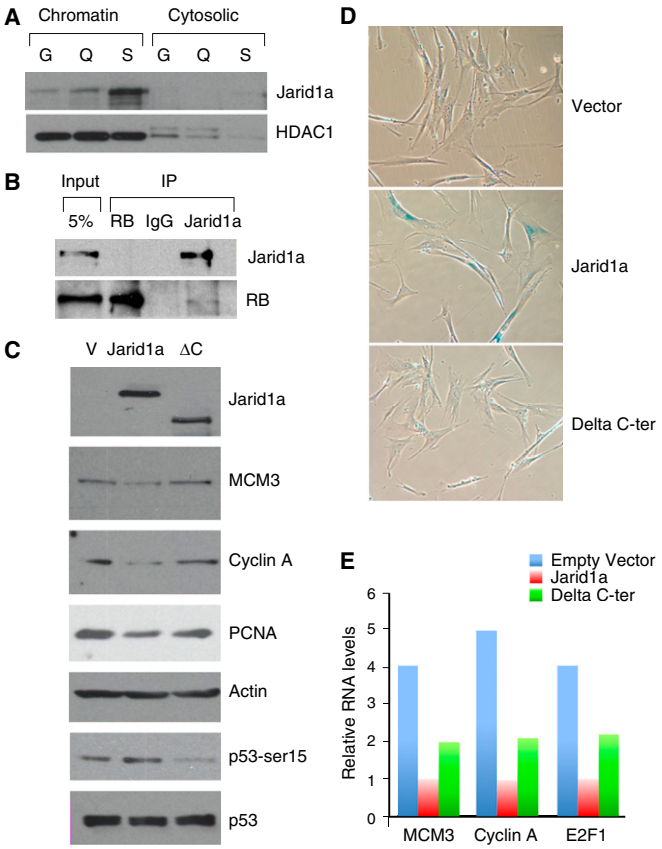

Fig. S3. (*A*) Immunoblots documenting the enrichment of Jarid1a in the chromatin-fraction of senescent cells. HDAC1 is used as loading control. (*B*) Immunoblots showing that RB coimmunoprecipitates with Jarid1a. Note, detection of Jarid1a in the RB immunoprecipitate is only detected at higher exposure (see Fig. 3). Higher exposure is not possible in this blot because we used anti-rabbit antibodies in both the immunoprecipitation and blotting steps, which leads to substantial background. (*C*) Immunoblots documenting the expression of C-terminal deletion mutant of Jarid1a and its effect on E2F target gene expression. Parallel blots were probed with an anti-actin antibody as a protein quantification control. (*D*) Micrograph showing the senescence marker SA-β-gal. Magnification: 20×. (*E*) Histogram showing the expression of E2F target genes in cells expressing either wild-type or the C-terminal deleted mutant Jarid1a.

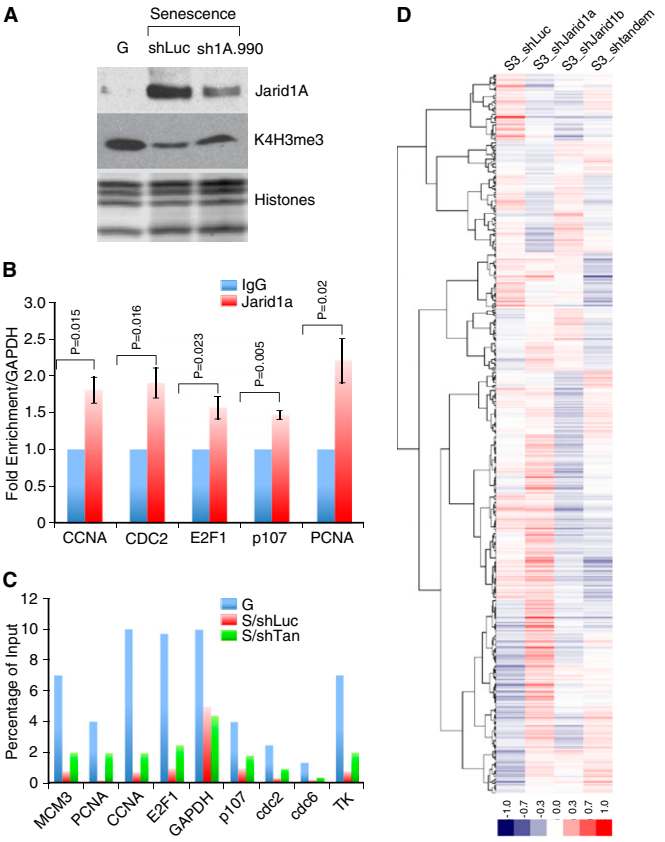

Fig. S4. (*A*) Immunoblots documenting the effectiveness of the shRNA targeting Jarid1a and its effect on H3K4me3 levels in senescent cells. Histones are shown as loading control. (*B*) Histogram showing the enrichment of Jarid1a at E2F target genes by ChIP analysis. Values represent the ± SE of at least three independent experiments. (*C*) Histogram documenting the relative levels of H3K4m3 at E2F target genes in growing (G), senescent (S/shLuc), or senescent cells expressing the tandem shRNAs targeting Jarid1a and Jarid1b (S/shTan). (*D*) Heatmap representing the relative expression of a subset of RB-regulated genes after suppression of Jarid1a, Jarid1b or both in senescent cells. Shown is the data for postselection day (PS) 3 (similar results are observed for PS7).

Dataset S1. Summary of qMS results

Dataset S1 (XLS)

Dataset S2. List of the H3K4me3 peaks identified in growing, quiescent, senescent, and shRB/senescent cells

Dataset S2 (XLS)

Dataset S3. Loci showing loss of H3K4me3 in senescent cells

Dataset S3 (XLSX)

Dataset S4. List of differentially expressed genes after suppression of Jarid1a, Jarid1b, or both in growing, quiescent, or senescent cells at PS3 and PS7

Dataset S4 (XLSX)

Dataset S5. Gene Ontology categories

Dataset S5 (XLSX)

Dataset S6. RB-regulated genes

Dataset S6 (XLSX)

Dataset S7. Jarid1a-regulated genes

Dataset S7 (XLSX)